Estimation of latent heat flux of pasture and maize in arid region of Northwest China based on canopy resistance modeling

Biyu Wang[1,2], Haofang Yan[1,3]*, Hexiang Zheng[2], Jiabin Wu[2], Delong Tian[2], Chuan Zhang[4], Xingye Zhu[1], Guoqing Wang[3], Imran Ali Lakhiar[1] and Youwei Liu[1]

[1]Research Center of Fluid Machinery Engineering and Technology, Jiangsu University, Zhenjiang, China, [2]Institute of Pastoral Hydraulic Research, China Institute of Water Resources and Hydropower Research, Hohhot, China, [3]State Key Laboratory of Hydrology-Water Resources and Hydraulic Engineering, Nanjing Hydraulic Research Institute, Nanjing, China, [4]Institute of Agricultural Engineering, Jiangsu University, Zhenjiang, China

Estimating the latent heat flux (λET) accurately is important for water-saving irrigation in arid regions of Northwest China. The Penman-Monteith model is a commonly used method for estimating λET, but the parameterization of canopy resistance in the model has been a difficulty in research. In this study, continuous observation of λET during the growing period of maize and grassland in Northwest China was conducted based on the Bowen ratio energy balance (BREB) method and the Eddy covariance system (ECS). Two methods, Katerji-Perrier (K-P) and Garcıá-Santos (G-A), were used to determine the canopy resistance in the Penman-Monteith model and the estimation errors and causes of the two sub-models were explored. The results indicated that both models underestimated the λET of grassland and maize. The K-P model performed relatively well ($R^2 > 0.94$), with the root mean square errors ($RMSE$) equaled 37.3 and 28.1 W/m² for grass and maize, respectively. The accuracy of the G-A model was slightly lower than that of the K-P model, with the determination coefficient (R^2) equaled 0.90 and 0.92, and the $RMSE$ equaled 46.2 W/m² (grass) and 42.1 W/m² (maize). The vapor pressure deficit (VPD) was the main factor affecting the accuracy of K-P and G-A sub-models. The error of two models increased with the increasing in VPD for both crops.

KEYWORDS

grassland, maize, heat flux, Northwest region, Penman-Monteith model

1 Introduction

As the inefficient utilization of water resources have become key constraints to eco-logically sustainable development, the development of reasonable irrigation systems is essential. Accurate determination of λET can provide a scientific basis for the development of a rational irrigation regime (Zhang et al., 2015; Niu et al., 2016; Yu, 2022). The λET is a important part of the energy balance and the water balance, which is closely related to the physiological activity of the crop and the harvested yield (Yan et al., 2023; Zheng et al., 2023). Substantial progress has been made by previous researchers on the actual measurement and simulation of λET (Yan et al., 2022b). Among them, the Penman-Monteith (P-M) model is one of the most commonly used methods to simulate λET. The

P-M model takes into account the effects of the canopy resistance (r_c) and the aerodynamic resistance (r_a) at the same time, and it can clearly reflect the process of evapotranspiration, which is the main model for the estimation of λET in a wide range of applications at the present time (Rana et al., 1997b; Yan et al., 2015). However, some of the parameters in the P-M model usually have uncertainties under different subsurface conditions, so the model parameters need to be corrected (Xu et al., 2020). The determination of r_c, which has a large impact on the estimation accuracy of the model, has been a difficult issue in research as well as in application. Many approaches have been developed to obtain the r_c, such as the Katerji-Perrier (K-P), Garciá-Santos (G-A), Todorovic (T-D), Jarvis and Leuning models (Katerji et al., 1983b; Todorovic, 1999; Li et al., 2014; Haofang et al., 2019; Guo et al., 2022). Accurately calculating r_c as a function of external factors is typically challenging. Katerji et al. (1983a) therefore propose a semi-empirical approach, where r_c depends on aerodynamic resistance and climate variables and its parameters need to be calibrated *in situ* (K-P model). The K-P model contains only 2 empirical coefficients and a large number of practices have found that the K-P model can be well applied to maize, grassland, soybean, sorghum, sunflower and other crops (Rana et al., 1994; Rana et al., 1997a; Todorovic, 1999; Rana et al., 2001; Lecina et al., 2003; Yan et al., 2022a). Todorovic (1999) created a mechanistic model for calculating λET that does not require *in situ* calibration, and the r_c is also dependent on aerodynamic resistance and climate variables (T-D model). According to Monteith (1965), the r_c can be calculated by dividing the minimal stomatal resistance by the leaf area that is participating in the energy exchange. The Jarvis model was developed by Jarvis (1976) and was widely used to explain how environmental conditions affect stomatal behavior. García-Santos et al. (2009) proposed a simplified r_c model (G-A model) by retaining only net radiation (R_n) and water vapor pressure difference (VPD) in the Jarvis-Stewart model, and the G-A model better simulated λET for trees, but it has not yet been applied in the estimation of λET for grassland and maize. García-Santos et al. (2009) indicated that the G-A model has better performance in arid regions. The G-A model is similar in complexity to the K-P model in that it contains 2 model parameters (Guo et al., 2022).

Liu et al. (2012) studied the performance of deriving time series of λET data for the crop of maize and canola in the lower part of the Murrumbidgee River Catchment in southeastern Australia and pointed out that the K-P method performed well, with the R^2 and $RMSE$ equaled 0.80–65.15 W/m^2, respectively. Gharsallah et al. (2013) conducted a preliminary study on the λET models for a surface irrigated maize agro-ecosystem in Italy, pointing out that the K-P model provides a good accuracy, with the R^2 and NSE equaled 0.73–0.76, respectively. Li (2019) used 10 canopy resistance sub-models such as K-P and G-A as the basis, and assessed the λET of maize in Baiyin City, Gansu Province through the P-M model, and the results showed that the K-P model gave more reliable results, and the G-A model had an overall error of 45.76% in 2 years, which made the simulation effect poorer. Yan et al. (2022a) conducted field observation experiments on summer maize and winter wheat in Southern Jiangsu Province, China, and found that both the K-P and T-D models could estimate the λET well, but the K-P model was more superior and the simulation results were more accurate compared to the T-D model for both crops. Lecina et al. (2003) experimented with the resistance for reference evapotranspiration

estimation in the Zaragoza and Co´rdoba, pointed out that the K-P model gave more reliable results. Li et al. (2015) conducted a preliminary study on the crop λET over the entire growing season in Wuwei City, Gansu Province of northwest China, pointing out that the G-A canopy resistance model after calibration has better accuracy in dense canopy phase. Guo et al. (2022) assessed the λET of winter wheat in northern China using six different models and observed significant improvements in the simulation results of the corrected G-A model compared to those prior to correction; after calibration, the models' effectiveness in estimating λET varied from excellent to good, ranked as follows: K-P, G-A, T-D, P-M, CO, and Jarvis. Among them, although the K-P and G-A models has been shown its good performance, the obtained model parameters in previous studies are not identical. Moreover, comparative studies of these two models in the same region as well as an analysis of the causes of errors in both models have rarely seen. Hence, experimental calibrations for the parameters for these models are needed based on more observation data from different fields, and a comparative study to evaluate the performance of the G-A and K-P methods is required in order to identify an appropriate approach for the specific field.

Water scarcity was a major problem in arid and semi-arid regions, constraining local agricultural and economic development. The Inner Mongolia Autonomous Region in northwestern China was a prime example of the urgent need to develop water-saving agricultural technologies. Northwest China, as an important agricultural reserve and strategic base for grain production (Deng, 2018), has a scarce precipitation (<500 mm of annual rainfall), and is characterized by arid, continental arid, semi-arid, and alpine climates (Guo et al., 2018). Irrigation water in the region is primarily derived from groundwater. Reductions in water diversions have made the task of determining accurate water consumption in the region even more urgent. Therefore, it is particularly important to determine precise irrigation regimes to minimize water wastage by accurately estimating the water consumption of major crops in the region. Despite many studies have conducted on the parameterization and validation of the P-M and canopy resistance models, the generalizability of the parameterization results and model accuracy still varies widely. Hence, the primary objective of this study is to assess the performance of λET simulated using the P-M model, by integrating the r_c sub-models (the K-P and G-A models), for two different vegetated covers (grass and maize) in the northwest area of China. The estimated λET were compared to the corresponding measured values using the Bowen ratio energy balance (BREB) and Eddy covariance system (ECS) methods. The causes of the discrepancies between the estimated and measured λET were analyzed. The optimal approach to estimate λET at the grassland and maize fields was recommended for establishing a more accurate irrigation scheduling. Analyzing the causes of estimation errors of the two models (the K-P and G-A models) in order to provide a scientific basis for predicting crop λET in arid regions.

2 Material and method

2.1 Experimental site

The experiments were conducted in a grassland and a maize field in 2020 and 2022, respectively. The grassland was located in

Yinshanbeilu Grassland Eco-hydrology National Observation and Research Station (N41°35′25″, E111°20′80″). The maize field was located in Chagan Sanshe, Suburga Township, Yijinholo Banner, respectively (N39°53′51″, E109°60′15″) (Figure 1).

The Yinshanbeilu Grassland Eco-hydrology National Observation and Research Station is located in the Damao Banner, Baotou City, Inner Mongolia. The total area of the research station is about 1.3 km², the altitude is 1,600 m, the annual mean temperature (T_a) of the location is 3.8°C, the annual mean wind speed is 5.3 m/s, the annual mean precipitation is 246 mm, the annual mean evaporation from the water surface is 2,200 mm, and the annual mean frost-free period is 110 days. The soils in the experimental site are chestnut soil. Due to differences in topography, parent material, water conditions, saline-alkali soil, and aeolian sand soil are formed in some areas. The overall amounts of potassium, phosphorus, and nitrogen in the soil were 2.5%, 0.08%–0.15%, and 0.1%–0.15%, respectively. Also, the pH of the soil ranged from 8 to 8.5. Grazing was the predominant land use, moderate-to-severe degradation had been widely distributed, and grassland overload in grazing regions was a major concern (Han et al., 2023).

The altitude of Suburga Township, Yijinholo Banner, Ordos City, is 1,456 m above sea level, the annual mean temperature (T_a) is 7.6°C, the average annual wind speed is 2.8 m/s, the average annual precipitation is 260 mm, the average annual evaporation from the water surface is 2,501 mm, and the average annual frost-free period is 160 days. The main crop grown in the area was maize. The climate type of the two areas is a mid-temperate and semi-arid continental monsoon climate and the soil texture is sandy loam.

2.2 Experimental details

The Krylov Needlegrass was the typical grassland group species in the Yinshanbeilu area, and the common species used were Artemisia frigida Willd, Leymus chinensis (Trin.) Tzvel., and Agropyron cristatum (L.) Gaertn (Han et al., 2022). The average height and coverage of vegetation was 40 cm and 35%, respectively (Miao et al., 2022). The growth periods of the grass in this study were divided into early (May 13–June 15), middle (June 15–August 15), and late stage (August 15–October 12).

Air temperature (T_a), relative humidity (RH), net radiation (R_n) and surface temperature (T_s) during grass growing season were measured by an ENVIS meteorological system (IMKO, Germany) at the Yinshanbeilu Grassland Eco-hydrology National Observation and Research Station. The meteorological observation instrument was installed at a height of 3.5 m. Air temperature and humidity sensors (HMP45C, Vasisla, Helsinki, Finland) were included, which were used to observe T_a and RH. In addition, R_n was observed by four-channel net radiation sensors (Kipp and Zonen, the Netherlands). The T_s was observed by an infrared radiometer (SI-111, Campbell Scientific, Inc., United States). The soil water content (SWC) at depths of 0–10 cm was measured. A tipping bucket rain gauge (TE525WS, Campbell Scientific Inc., United States) was used to measure precipitation (P) and stored after calculating the average

value for 30 min. The Eddy covariance system (ECS) used in this study was manufactured by Licor Corporation, United States. The system mainly consisted of a three-dimensional ultrasonic anemometer (CSAT-3, Campbell Scientific, Logan, UT, United States), an infrared gas analyzer (LI-7500, Li-CORInc, United States), integrate, short and longwave radiation in one sensor (NR-LITE, Campbell Scientific), two soil heat flux plates, which were buried about 10 cm below the ground surface (HFP01, Campbell Scientific). The data acquisition (CR3000, Campbell Scientific) was at a frequency of 10 Hz with a measurement step of 30 min (8:00–18:00).

Maize (Fengtian 1,631) in Yijinholo Banner was planted in 1 May 2022 and harvested in 30 September 2022 with a planting density of 5,600 plants/acre. The experiment was conducted using a single-wing labyrinth drip irrigation laterals with 0.3 m emitter spacing, emitter flow rate of 3.6 L/h and wall thickness of 0.4 mm. The drip irrigation pipes were buried at 3–5 cm under the soil surface.

An automated weather station was installed in the middle of the maize field. Net radiation (R_n) was measured by a CNR-4 sensor (Kipp and Zonen, the Netherlands) at 3 m above ground. Air temperature and relative humidity were recorded with psychrometers HMP155A (Vaisala, Finland) at a height of 3 and 4 m above ground. The infrared thermometer (SI-111, Apogee, United States) was adjusted to the height of the crop canopy during the experiment and continuously measured the crop canopy temperature. Wind speed and direction were measured by a three cups anemometer A100L2 (MetOne, United States) at 3 m above ground. Soil heat flux was measured with a soil heat flux plate HFP01-L10 (Campbell Scientific, United States). All the sensors were connected to a data logger CR3000 (Campbell Scientific, United States) and all the data were sampled every 10 s, averaged every 10 min. The accuracy of all the sensors was validated before the installation. The maize field was surrounded by other similar crops and the installation height of the probes used to observe the air temperature and relative humidity was low (50–100 cm above the canopy), so, adequate fetch length can be met.

2.3 Methods

The energy balance equation could be expressed as Eq. 1 (Shi et al., 2021):

$$R_n - G = \lambda ET + H \tag{1}$$

where, R_n is net radiation (W/m²), G is soil heat flux (W/m²), λET is latent heat flux (W/m²), H is sensible heat flux (W/m²).

Hourly latent heat flux of maize was obtained by the Bowen ratio energy balance (BREB) method (Yan et al., 2021) given by Eq. 2:

$$\lambda ET = \frac{R_n - G}{1 + \beta} \tag{2}$$

where, β is the Bowen ratio and can be expressed as Eq. 3:

$$\beta = \frac{H}{\lambda ET} = \lambda \frac{\Delta T}{\Delta e} \tag{3}$$

FIGURE 1
Location of the study area.

FIGURE 2
The energy balance ratio in May−October 2020.
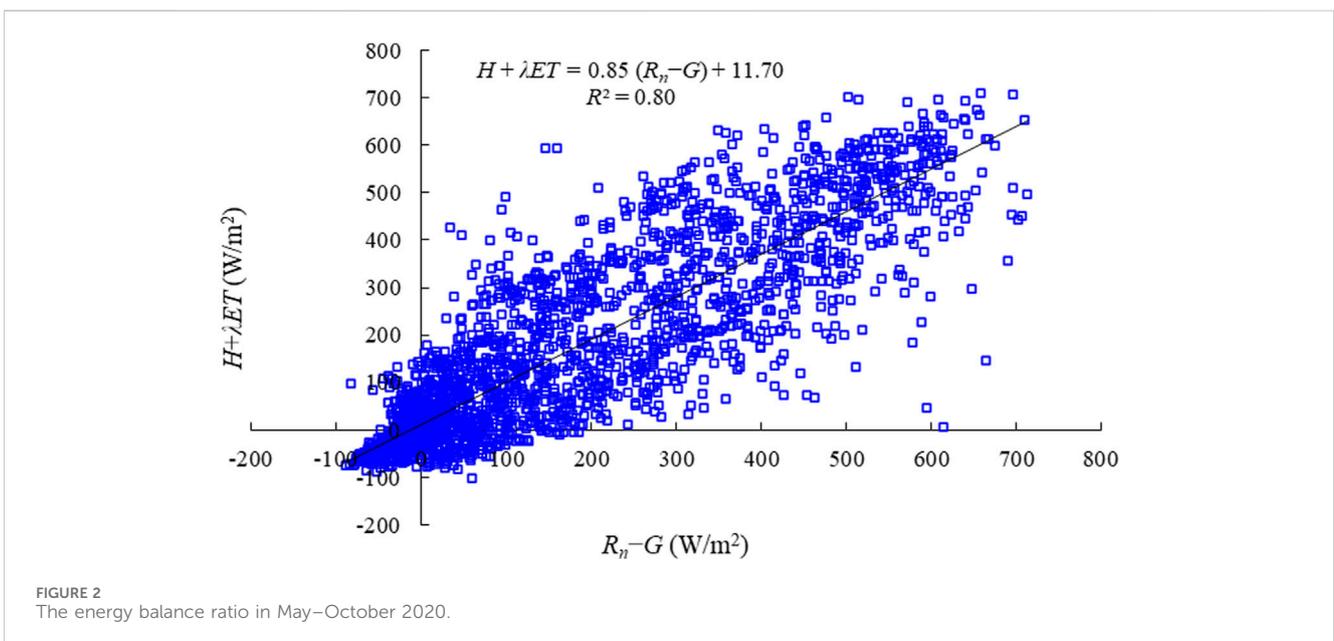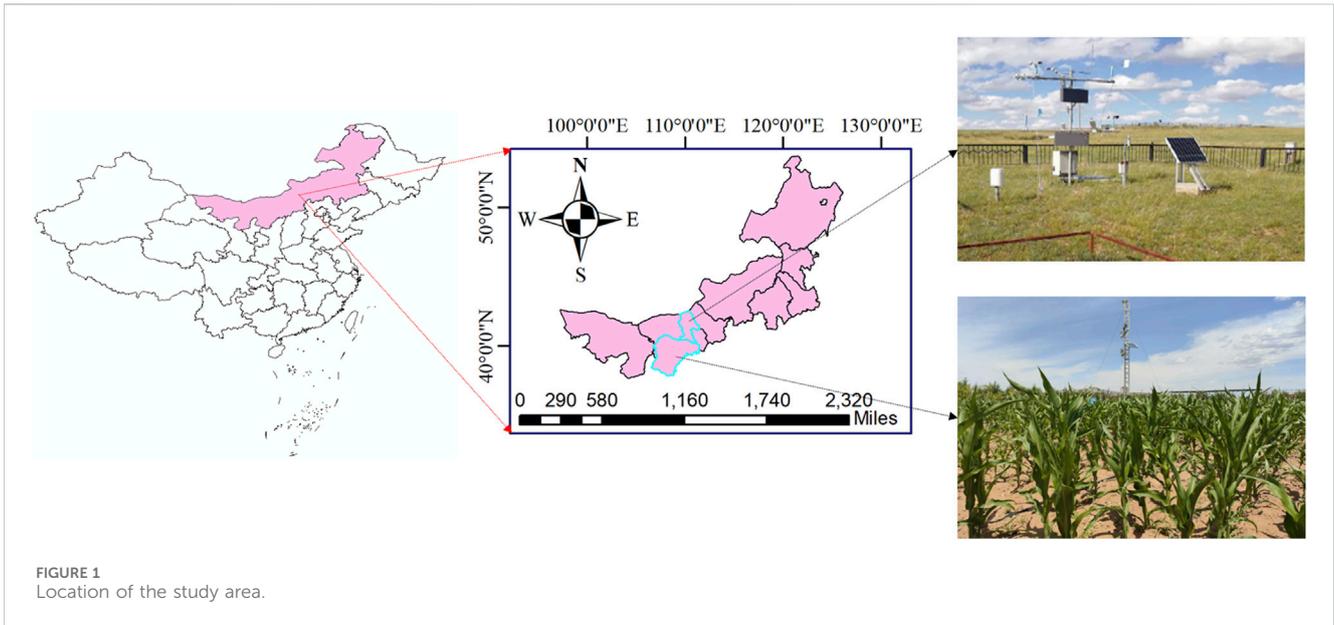
where, ΔT is the air temperature gradient, Δe is the actual vapor pressure gradient and λ is the psychrometric constant (kPa/°C).

Hourly λET of grassland was obtained by the Eddy covariance system (ECS).

The latent heat flux (λET) was calculated from the covariance between the vertical wind speed and the water vapor concentration, as shown in Eq. 4:

$$\lambda ET = \rho C_p \overline{w'q'} \qquad (4)$$

where, λET represents the latent heat flux (W/m²), ρ represents the air density (kg/m³), C_p is the specific heat of air (J/(kg·°C)), and w' and q' represent the pulsations of the vertical wind speed and water vapor content, respectively.

Energy balance closure analysis of the ECS is one of the main methods for analyzing the reliability of flux data, the energy balance ratio (*EBR*) was determined using Eq. 5:

$$EBR = \frac{\sum(\lambda ET + H)}{\sum(R_n - G)} \times 100\% \qquad (5)$$

where, *EBR* denotes the energy closure (%), G denotes the soil heat flux (W/m²), H denotes the sensible heat flux (W/m²), and R_n denotes the net radiation (W/m²).

The *EBR* during the observation period (May- October 2020) was approximately 85% (Figure 2). Li et al. (2018) analyzed the site energy closure of the Chinese flux network with R^2 ranging from 0.51 to 0.93 and regression slopes from 0.54 to 0.88. The energy closure of this site is in a reasonable range compared to data from other sites.

2.4 Model description

2.4.1 Penman-Monteith model

The λET were calculated by the Penman-Monteith (P-M) model (Monteith, 1965) as Eq. 6:

$$\lambda ET = \frac{\Delta(R_n - G) + \rho_a C_p \frac{VPD}{r_a}}{\Delta + \gamma\left(1 + \frac{r_c}{r_a}\right)} \tag{6}$$

where, VPD is the water vapor pressure difference (kPa), ρ_a is the density of air at atmospheric pressure (kg/m³), C_p is the specific heat of air [J/(kg·°C)], Δ is the slope of the curve relating saturated water vapor pressure and temperature (kPa/°C), r_c is the canopy resistance parameter (s/m), r_a is the aerodynamic resistance (s/m).

The r_a was calculated by applying the logarithmic function of the wind speed. The equation (Perrier, 1975) are Eqs 7–9:

$$r_a = \frac{\ln\frac{z-d}{z_0}\ln\frac{z-d}{h_c-d}}{K^2 u_z} \tag{7}$$

$$z_0 = 0.123 h_c \tag{8}$$

$$d = 0.67 h_c \tag{9}$$

where, K is the von Karman constant (=0.41), z is the height of wind measurements (m), d is the zero plane displacement height (m), u_z is the wind speed at height z (m/s), h_c is the mean height of the crop (m).

2.4.2 Katerji-Perrier model

Katerji et al. (1983b) developed a linear relationship between the ratios r_c/r_a and $r*/r_a$ with the following relation (K-P model), as shown in Eq. 10:

$$\frac{r_c}{r_a} = a\frac{r^*}{r_a} + b \tag{10}$$

where, a and b are empirical coefficients, r^* is climatic resistance (s/m) and defined as Eq. 11:

$$r^* = \frac{\Delta + \gamma}{\Delta\gamma}\frac{\rho C_p VPD}{R_n - G} \tag{11}$$

While the K-P method and the P-M equation share similar hypotheses, the K-P method makes the assumption that the ae rodynamic resistance originates from the top of the canopy and that the "big leaf" is situated there. Thus, the following is a suggested aerodynamic resistance (Rana et al., 2005), as shown in Eq. 12.

$$r_a = \frac{\ln\frac{z-d}{z_0}\ln\frac{z-d}{h_c-d}}{k^2 u_z} \tag{12}$$

where, h_c is the reference crop height in this paper, z_0 is the roughness length estimated as $z_0 = 0.1 h_c$, d is the zero plane displacement estimated as $d = 0.67 h_c$, z is the height of measurements (m), u_z is the wind speed at the height of z (m/s).

2.4.3 Garcıá-Santos model

The Garcıá-Santos (G-A) model is based on the Jarvis-Stewart model that calculates hourly canopy conductance. Only the R_n and VPD were considered in the model. The G-A canopy resistance model is expressed as follows (García-Santos et al., 2009):

$$\frac{1}{r_c} = g_{sm}\left(\frac{(1100 + e_1)R_n}{1100(R_n + e_1)}\right)\exp(-e_2 VPD) \tag{13}$$

where, g_{sm} (mm/s), e_1 (W/m²) and e_2 (g/kg) are empirical coefficients which need experimental determination, VPD is the vapor pressure deficit (kPa).

2.5 Statistical evaluation

The statistical indices include the determination coefficient (R^2), mean absolute error (MAE), Nash-Sutcliffe Efficiency (NSE) and root mean square error ($RMSE$), defined as shown in Eqs 14–16:

$$MAE = \frac{1}{n}\sum_{i=1}^{n}|E_i - O_i| \tag{14}$$

$$RMSE = \sqrt{\frac{1}{n}\sum_{i=1}^{n}(E_i - O_i)^2} \tag{15}$$

$$NSE = 1 - \frac{\sum_{i=1}^{n}(E_i - O_i)^2}{\sum_{i=1}^{n}(O_i - \bar{O})^2} \tag{16}$$

where, E_i represent the estimated values, O_i represent the observed values, O is the mean of observed values, n is the total number of semple.

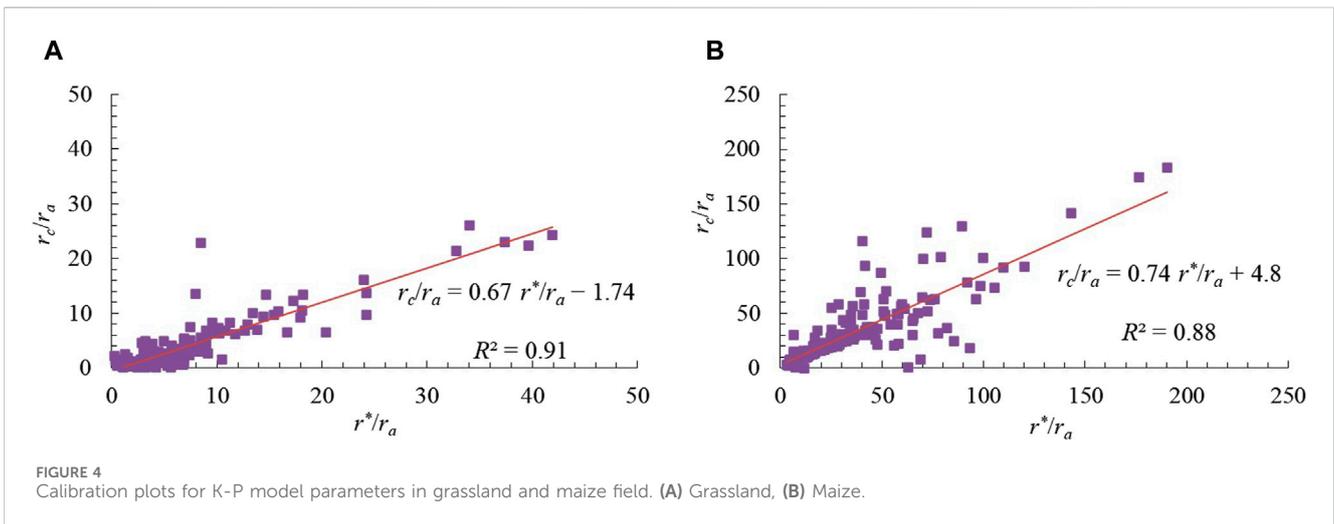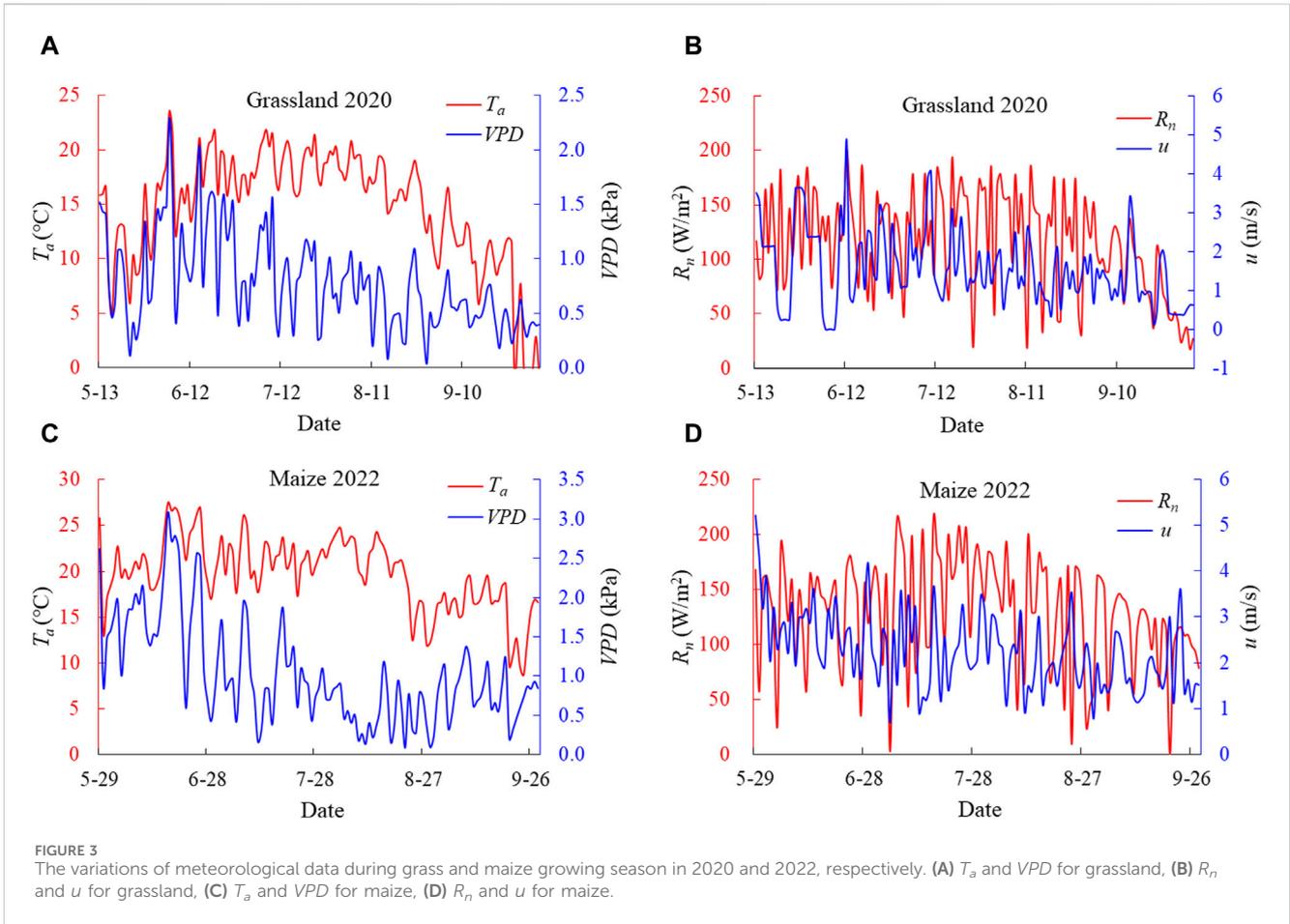# 3 Results

3.1 Meteorological data

The observed meteorological data during the growing periods of grass and maize plants are shown in Figure 3. The air temperature (T_a) and vapor pressure deficit (VPD) during grass growing season in 2020 (from 13 May 2020 to 5 October 2020) ranged from −4.49°C to 23.60°C and 0.04–2.29 kPa, with average values equaled 14.74°C and 0.78 kPa, respectively. Daily R_n ranged from 19.2 to 200.4 W/m², with mean value of 116.1 W/m². The daily wind speed (u) varied from 0.12 to 4.87 m/s, with the highest value of 4.87 m/s in the summer season.

The T_a and VPD ranged from 8.71°C to 27.53°C and 0.09–3.08 kPa, with average values equaled 19.79°C and 1.03 kPa during maize growing season in 2022 (from 29 May 2022 to 28 September 2022). Daily R_n ranged from 0.17 to 216.31 W/m², with mean value of 129.95 W/m². The value of u varied from 0.69 to 5.20 m/s, with mean value of 2.24 m/s.

3.2 Estimation of latent heat flux

3.2.1 Calibration of the Katerji-Perrier model

The K-P model was calibrated based on the data from grassland and maize fields individually. The model coefficients a and b were yielded from the linear regression between r_c/r_a and $r*/r_a$ for each site. In this study, the K-P model was calibrated using hourly data during ten typical clear days, which were randomly chosen from the experimental periods at the grassland and maize fields. The r_c was computed by inverting

FIGURE 3
The variations of meteorological data during grass and maize growing season in 2020 and 2022, respectively. **(A)** T_a and VPD for grassland, **(B)** R_n and u for grassland, **(C)** T_a and VPD for maize, **(D)** R_n and u for maize.

FIGURE 4
Calibration plots for K-P model parameters in grassland and maize field. **(A)** Grassland, **(B)** Maize.

the Eq. 6 with the measured λET. The Figure 4, Eqs 17, 18 represent the results of the linear regression between the r_c/r_a and r^*/r_a for the grassland and maize. The regression coefficients a and b of the K-P model were 0.67 and −1.74 for grassland and 0.74 and 4.8 for maize, respectively. The determination coefficients (R^2) were 0.91 and 0.88 for grassland and maize, respectively. Moreover, the results of some previous studies for

the calibration results of the K-P model are summarized as shown in Table 1.

$$\frac{r_c}{r_a} = 0.67\frac{r^*}{r_a} - 1.74, R^2 = 0.91 \tag{17}$$

$$\frac{r_c}{r_a} = 0.74\frac{r^*}{r_a} + 4.8, R^2 = 0.88 \tag{18}$$

TABLE 1 Summary of the calibration coefficients a and b of the K-P model for different study areas or crops conducted by previous studies.

Crop	a	b	R^2	Experimental sites	References
Tea	1.05	0.30	0.96	Zhenjiang, Jiangsu	Yan et al. (2021)
Wheat	0.59	0.12	0.91	Zhenjiang, Jiangsu	Yan et al. (2021)
Grass	0.16	0.00	0.59	Southern Italy	Rana et al. (1994)
Sunflower	0.45	0.20	0.60	Southern Italy	Rana et al. (1997a)
Lettuce	0.73	−0.58	0.97	South-central Portugal	Alves and Pereira (2000)
Tomato	0.54	2.40	0.55	Southern Italy	Rana et al. (1997a)
Canola	0.09	0.13	0.23	Southeastern Australia	Liu et al. (2012)
Grain sorghum	0.54	0.61	0.43	Southern Italy	Rana et al. (1997a)
Sweet sorghum	0.85	1.00	0.92	Southern Italy	Rana et al. (1997a)
Soybean	0.95	1.55	0.69	Southern Italy	Rana et al. (1997a)
Oats	0.88	3.39	0.42	Southern Italy	Rana et al. (2011)
Vineyard	0.91	0.45	0.78	Southern Italy	Katerji et al. (2011)
Canola	0.09	0.13	0.23	Southeastern Australia	Liu et al. (2012)
Maize	1.50	−1.72	0.25	Southeastern Australia	Liu et al. (2012)
Maize	0.24	4.44	–	Northern Italy	Gharsallah et al. (2013)

TABLE 2 Optimized values of parameters (g_{sm}, e_1, e_2) in the G-A model and the variance explained by the model for grassland and maize.

Crop	g_{sm} (mm/s)	e_1 (W/m²)	e_2 (g/kg)	Variance explained (%)
Grassland	0.38	1742	6.20	79.1
Maize	0.56	1987	8.13	82.4

TABLE 3 Summary of calibration coefficients g_{sm}, e_1 and e_2 of the G-A model for different crops of previous studies.

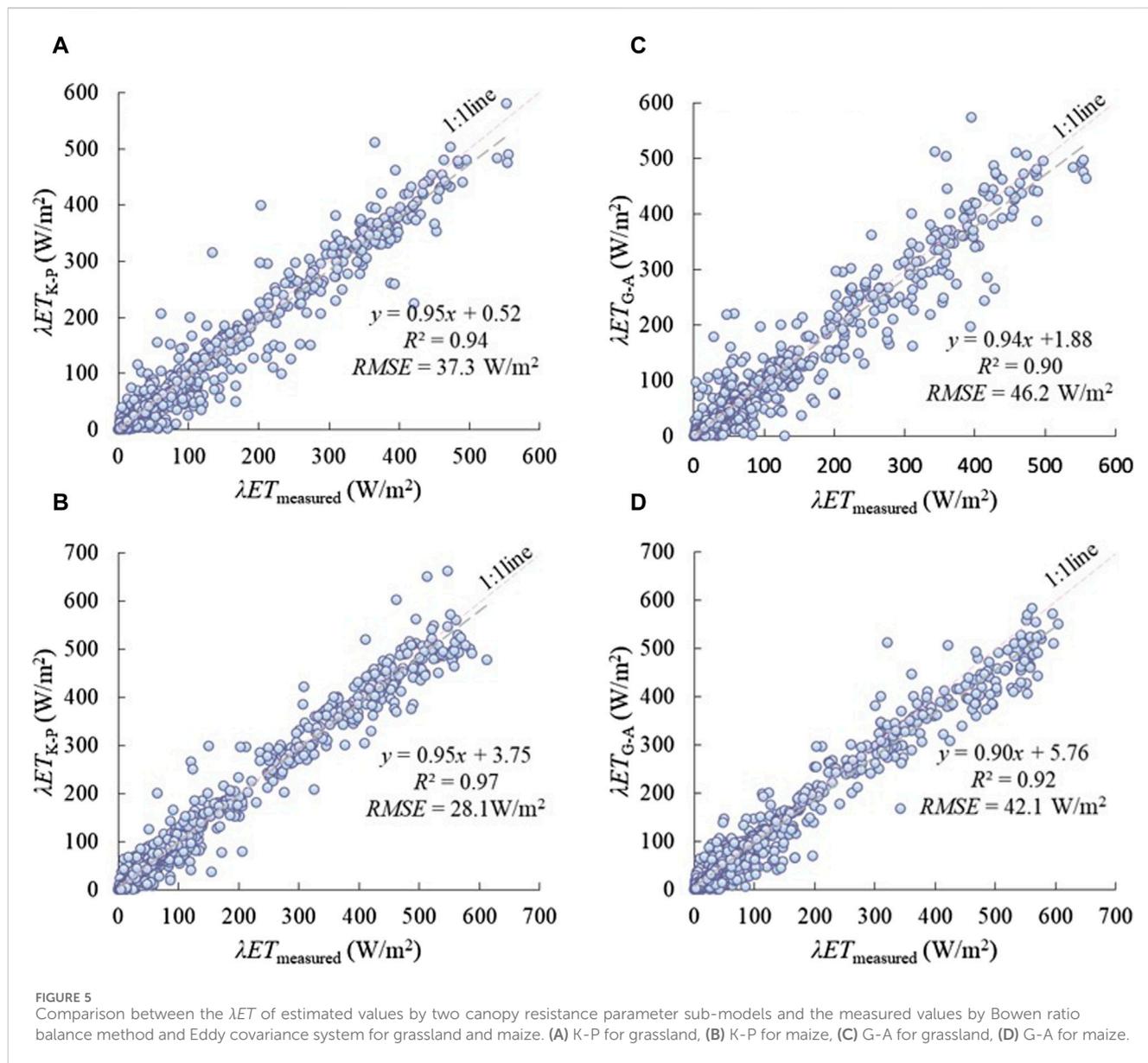| Crop	g_{sm} (mm/s)	e_1 (W/m²)	e_2 (g/kg)	Experimental sites	References
Maize	0.34	1,589.1	2.132	Baiyin, Gansu	Li (2019)
Wheat	4.81	514.82	0.906	Beijing	Guo et al. (2022)
Rainy season forests	11.80	433.10	0.084	Canary Islands, Spain	García-Santos et al. (2009)
Dry season forests	6.30	280.00	0.046	Canary Islands, Spain	García-Santos et al. (2009)

3.2.2 Calibration of the Garcıá-Santos model

The parameters of G-A model were calibrated using the least squares method through hourly scale data from ten typical clear days. The basic principle of the least squares method is to estimate the model parameters on the criterion of minimizing the sum of squares of the errors. Data for the days used to calibrate the model were not used for the validation of modeled r_c and λET. The r_c was computed by inverting the Eq. 6 with the measured λET. The optimized parameters g_{sm} (mm/s), e_1 (W/m²) and e_2 (g/kg) as well as the degree of variance explained (%) by the model for grasslands and maize are listed in Table 2.

The results of some previous studies for the calibration results of the G-A model are summarized as shown in Table 3.

3.3 Evaluation of the canopy resistance model

For the K-P model, the slope of the linear relationships between estimated and measured λET values was 0.95 for grassland and 0.97 for maize during the whole growing period (Figures 5A, B). Thus, the K-P model underestimated λET slightly both in the cases of grassland and maize. The intercepts were 0.52 and 3.75, with $RMSE$ of 37.3 and 28.1 W/m² for grassland and maize, respectively.

For the G-A model, the slope of the linear relationships between estimated and measured λET was 0.94 for the grassland (Figure 5C) with $RMSE$ of 46.2 W/m² and NSE of 0.88, indicating that the G-A model underestimated the λET significantly, while the slope was

FIGURE 5
Comparison between the λET of estimated values by two canopy resistance parameter sub-models and the measured values by Bowen ratio balance method and Eddy covariance system for grassland and maize. **(A)** K-P for grassland, **(B)** K-P for maize, **(C)** G-A for grassland, **(D)** G-A for maize.

0.92 for the maize (Figure 5D) with *RMSE* of 42.1 W/m² and *NSE* of 0.90.

According to the statistics presented in Table 4, the best *NSE* value (=0.96) was obtained with the K-P model for maize. The worst *NSE* value (=0.88) was obtained with the G-A model for grassland, despite the G-A model giving an excellent *NSE* value of 0.90 for maize. The best *MAE*, acquired on maize for K-P method, was equal to 19.3 W/m².
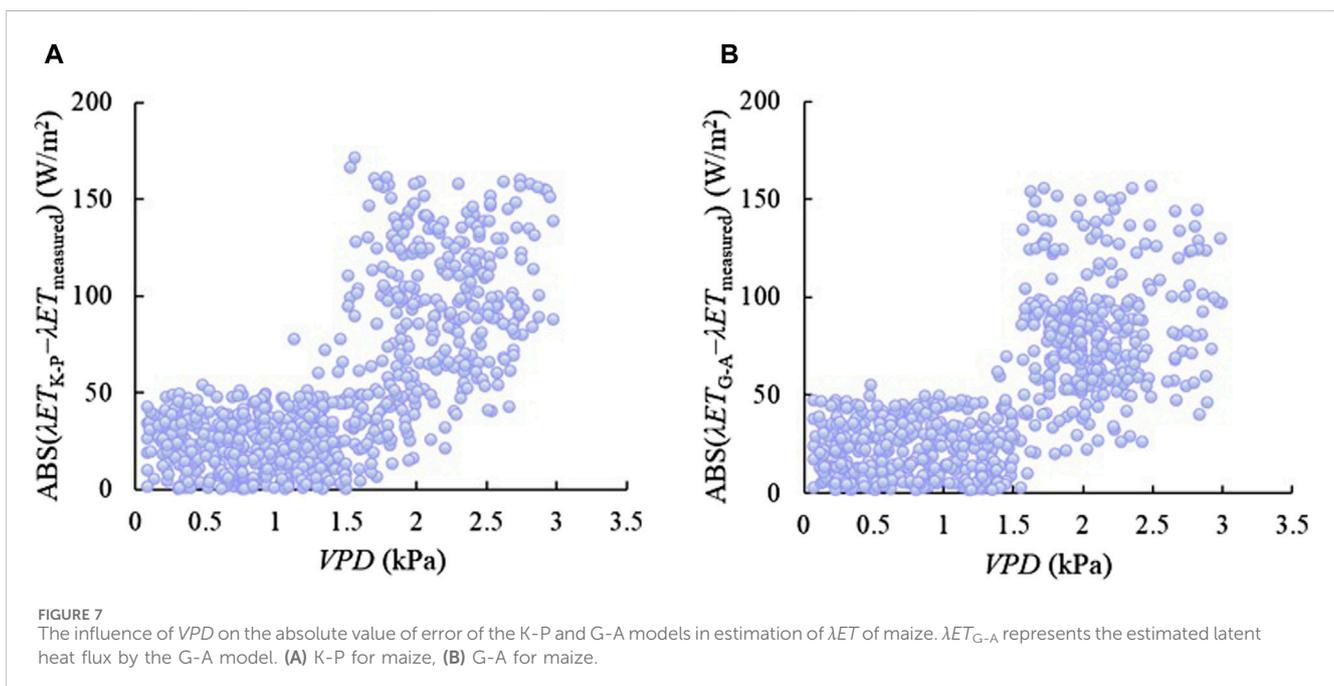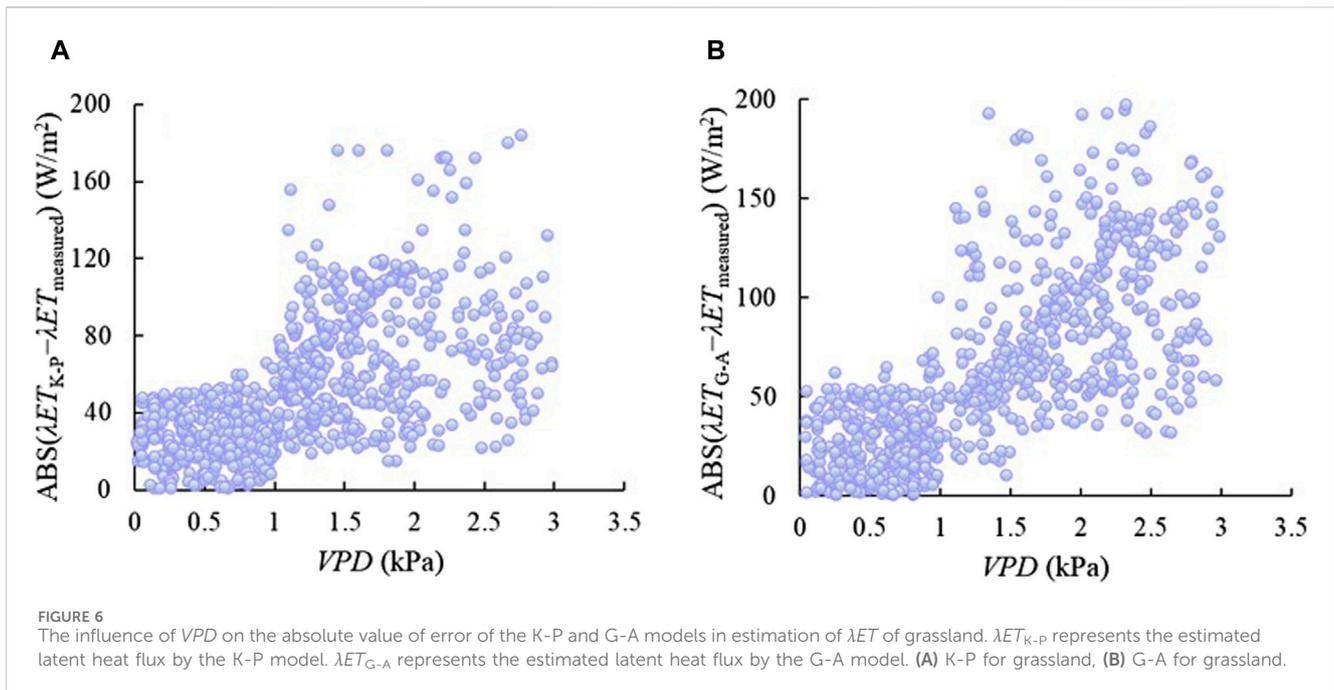
TABLE 4 Statistical indices between estimated and measured λET of grassland and maize field.

Crop type	Model	MAE (W/m²)	RMSE (W/m²)	NSE
Grassland	K-P	25.2	37.3	0.93
	G-A	30.8	46.2	0.88
Maize	K-P	19.3	28.1	0.96
	G-A	27.6	42.1	0.90

4 Discussion

In this study, the K-P and G-A models were used to simulate the λET based on the P-M model during the growing periods of grass and maize in the arid region of Northwest China. The estimated λET values of the K-P and G-A model (λET_{K-P} and λET_{G-A}) were smaller than the measured λET for grassland. The possible reason might due

to the effects of changes in soil moisture and crop *LAI* on canopy resistance during the growing periods were not taken into account. Li et al. (2015) conducted experimental studies on maize and grape in the northern region of China based on twelve r_c models, and the results showed that the K-P model simulation results were more superior. Simulations of λET in olive trees by Margonis et al. (2018)

FIGURE 6
The influence of *VPD* on the absolute value of error of the K-P and G-A models in estimation of λET of grassland. λET_{K-P} represents the estimated latent heat flux by the K-P model. λET_{G-A} represents the estimated latent heat flux by the G-A model. **(A)** K-P for grassland, **(B)** G-A for grassland.

FIGURE 7
The influence of *VPD* on the absolute value of error of the K-P and G-A models in estimation of λET of maize. λET_{G-A} represents the estimated latent heat flux by the G-A model. **(A)** K-P for maize, **(B)** G-A for maize.

showed that the K-P model underestimated λET by about 9.8%. The results of all the above studies were consistent with the results of the present study.

The relationships between meteorological factors and absolute value of error of the K-P and G-A models in estimating λET were analyzed, it was found that *VPD* was the main factor affecting the model errors (Figure 6), while other factors have little influence. For the grassland, when the *VPD* value exceeds 1 kPa, the error increased with the increasing in *VPD* for both models. Shi et al.

(2008) experimented with the broad-leaved Korean pine forest in the Changbai Mountains in the south-east of Jilin Province, China, pointed out that when the value of *VPD* was more than 1.5 kPa, the accuracy of estimation tended to below.

For the maize field, when the *VPD* exceeded 1.5 kPa, the absolute value of error increased with the increasing in *VPD* (Figure 7). Results similar to this study were reported by Katerji et al. (2011) on the effect of *VPD* in the values of evapotranspiration which stated that when the value of *VPD*

was more than 2 kPa, the values of the estimated evapotranspiration were larger than the measured evapotranspiration. The greater abundance of water vapor in July and August in maize field may be another reason for the underestimation of λET by the K-P model. Most of the $\lambda ET_{\text{G-A}}$ were smaller than the $\lambda ET_{\text{measured}}$ during the growing period of maize especially when the $\lambda ET_{\text{measured}}$ was high. Srivastava et al. (2018) conducted a preliminary study on the effect of VPD in the value of evapotranspiration in the West Bengal, India, pointing out that when the value of VPD was in the range of 1.23–3.0 kPa, the accuracy of estimation tended to below. The more abundant water vapor in the maize field in July and August may also contributed to the large errors in the simulation results of the G-A model simulation results.

Generally, the K-P model were more accurate in simulating the λET of grassland and maize field in Northwest China.

5 Conclusion

In this study, two r_c models (K-P and G-A) were applied and compared for the λET estimation. Based on the analysis of statistical indices, the following conclusions were made.

The K-P model was the superior method for predicting hourly λET of grassland and maize. The G-A model was a good alternative approach for estimating λET of grassland and maize. For the K-P model, the $RMSE$ were equal 37.3–28.1 W/m^2 for grassland and maize, respectively. For the G-A model, the $RMSE$ values was 46.2 W/m^2 for grassland and 42.1 W/m^2 for maize during the whole growing period. The results showed that the R^2 of the simulation results of the two r_c models (K-P and G-A) were above 0.8, but the K-P model simulation was better. Both the K-P and G-A models underestimated the λET of grassland and maize.

The absolute error of the two models increased with the increasing in VPD. For the K-P model, the effect of LAI changes on crop canopy resistance during crop growth was not considered, which would have made the model performance slightly worse in the early part of the growing season. For the G-A model, due to the limitations of the modeling theory, only the effects of mete-orological factors such as R_n and VPD were taken into account, while the effect of soil on evapotranspiration was not considered, which would have made the model performance slightly worse (Li et al., 2015). Matheny et al. (2014)conducted a preliminary study on the prediction of evapotranspiration in the North Ameri-can, pointing out that most r_c models under water stress conditions have difficulty in re-

solving the dynamics of λET due to errors in calculating surface resistance.

Data availability statement

The original contributions presented in the study are included in the article/supplementary material, further inquiries can be directed to the corresponding author.

Author contributions

BW: Writing–original draft. HY: Writing–review and editing. HZ: Funding acquisition, Writing–review and editing. JW: Writing–review and editing. DT: Writing–review and editing. CZ: Writing–review and editing. XZ: Writing–review and editing. GW: Writing–review and editing. IL: Writing–review and editing. YL: Writing–review and editing.

Funding

Conflict of interest

The authors declare that the research was conducted in the absence of any commercial or financial relationships that could be construed as a potential conflict of interest.

Publisher's note

References

Alves, I., and Pereira, L. S. (2000). Modelling surface resistance from climatic variables? *Agric. Water Manag.* 42 (3), 371–385. doi:10.1016/s0378-3774(99)00041-4

Deng, M. (2018). *"Three Water Lines" strategy: its spatial patterns and effects on water resources allocation in northwest China.*

García-Santos, G., Bruijnzeel, L. A., and Dolman, A. J. (2009). Modelling canopy conductance under wet and dry conditions in a subtropical cloud forest. *Agric. For. Meteorology* 149 (10), 1565–1572. doi:10.1016/j.agrformet.2009.03.008

Gharsallah, O., Facchi, A., and Gandolfi, C. (2013). Comparison of six evapotranspiration models for a surface irrigated maize agro-ecosystem in Northern Italy. *Agric. Water Manag.* 130, 119–130. doi:10.1016/j.agwat.2013.08.009

Guo, B., Kong, W. H., and Jiang, L. (2018). Dynamic monitoring of vulnerability and quantitative analysis of driving factors in northwest arid desert ecosystem. *Nat. Resour.* 33, 412–424. doi:10.11849/zrzyxb.20170068

Guo, Z., Wu, Y., Li, Q., Gu, F., Liu, X., Li, Y., et al. (2022). Application of six canopy resistance models for estimating winter wheat evapotranspiration. *Trans. Chin. Soc. Agric. Eng.* 38 (12), 109–117. doi:10.11975/j.issn.1002-6819.2022.12.013

Han, X., Zhang, B. Z., Liu, T. J., Wang, J., Zhou, Q. Y., and Che, Z. (2023). The effect of time scales on the distribution of evapotranspiration and driving factors in desert grasslands. *Agric. Water Manag.* 284, 108348. doi:10.1016/j.agwat.2023. 108348

Han, X., Zhou, Q. Y., Zhang, B. Z., Che, Z., Wei, Z., Qiu, R. J., et al. (2022). Real-time methods for short and medium-term evapotranspiration forecasting using dynamic crop coefficient and historical threshold. *J. Hydrology* 606, 127414. doi:10.1016/j. jhydrol.2021.127414

Haofang, Y., Baoshan, Z., Chuan, Z., Song, H., Hanwen, F., Jianjun, Y., et al. (2019). Estimating cucumber plants transpiration by Penman-Monteith model in Venlo-type greenhouse. *Trans. Chin. Soc. Agric. Eng.* doi:10.11975/j.issn.1002-6819.2019.08.018

Jarvis, P. (1976). The interpretation of the variations in leaf water potential and stomatal conductance found in canopies in the field. *Philosophical Trans. R. Soc. Lond. B, Biol. Sci.* 273 (927), 593–610. doi:10.1098/rstb.1976.0035

Katerji, N., Perrier, A., and Oulid-Aïssa, A. K. (1983a). Exploration au champ et interprétation de la variation horizontale et verticale de la résistance stomatique: cas d'une culture de luzerne (Medicago sativa L.). *Agronomie* 3 (9), 847–856. doi:10.1051/ agro:19830904

Katerji, N., Perrier, A., Renard, D., and Aissa, A. K. O. (1983b). Modélisation de l'évapotranspiration réelle ETR d'une parcelle de luzerne: rôle d'un coefficient cultural. *Agronomie* 3 (6), 513–521. doi:10.1051/agro:19830603

Katerji, N., Rana, G., and Fahed, S. (2011). Parameterizing canopy resistance using mechanistic and semi-empirical estimates of hourly evapotranspiration: critical evaluation for irrigated crops in the Mediterranean. *Hydrol. Process.* 25 (1), 117–129. doi:10.1002/hyp.7829

Lecina, S., Martínez-Cob, A., Pérez, P. J., Villalobos, F. J., and Baselga, J. J. (2003). Fixed versus variable bulk canopy resistance for reference evapotranspiration estimation using the Penman-Monteith equation under semiarid conditions. *Agric. Water Manag.* 60 (3), 181–198. doi:10.1016/s0378-3774(02)00174-9

Li, L. (2019). *Application of different canopy resistance models to evapotranspiration in maize ecosystems in semi-arid areas*. Lanzhou University.

Li, S. E., Hao, X. M., Du, T. S., Tong, L., Zhang, J. H., and Kang, S. Z. (2014). A coupled surface resistance model to estimate crop evapotranspiration in arid region of northwest China. *Hydrol. Process.* 28 (4), 2312–2323. doi:10.1002/hyp.9768

Li, S. E., Zhang, L., Kang, S. Z., Tong, L., Du, T. S., Hao, X. M., et al. (2015). Comparison of several surface resistance models for estimating crop evapotranspiration over the entire growing season in arid regions. *Agric. For. Meteorology* 208, 1–15. doi:10. 1016/j.agrformet.2015.04.002

Li, Z., Yu, G., and Wen, X. (2018). Evaluation of the energy balance closure status of the China flux observation network (ChinaFLUX). *Sci. China Series D Earth Sci.* 2004 (S2), 46–56.

Liu, G. S., Liu, Y., Hafeez, M., Xu, D., and Vote, C. (2012). Comparison of two methods to derive time series of actual evapotranspiration using eddy covariance measurements in the southeastern Australia. *J. Hydrology* 454, 1–6. doi:10.1016/j. jhydrol.2012.05.011

Margonis, A., Papaioannou, G., Kerkides, P., Kitsara, G., and Bourazanis, G. (2018). Canopy resistance and actual evapotranspiration over an olive orchard. *Water Resour. Manag.* 32 (15), 5007–5026. doi:10.1007/s11269-018-2119-x

Matheny, A. M., Bohrer, G., Stoy, P. C., Baker, I. T., Black, A. T., Desai, A. R., et al. (2014). Characterizing the diurnal patterns of errors in the prediction of evapotranspiration by several land-surface models: an NACP analysis. *J. Geophys. Research-Biogeosciences* 119 (7), 1458–1473. doi:10.1002/2014jg002623

Miao, H. L., Wang, A. T., Zhang, R. Q., Li, J. R., and Gao, T. M. (2022). Characteristics of wind regime and drift potential of the desert steppe in northern slope of Yinshan Mountains. Inner Mongolia. *J. Arid Land Resour. Environ* 36, 102–110. doi:10.13448/j. cnki.jalre.2022.098

Monteith, J. L. (1965). Evaporation and environment. *Symposia Soc. Exp.* 19, 205–234.

Niu, G., Li, Y. P., Huang, G. H., Liu, J., and Fan, Y. R. (2016). Crop planning and water resource allocation for sustainable development of an irrigation region in China under multiple uncertainties. *Agric. Water Manag.* 166, 53–69. doi:10.1016/j.agwat.2015. 12.011

Perrier, A. (1975). *Etude physique de l'évapotranspiration dans les conditions naturelles. III*. Evapotranspiration réelle et potentielle des couverts végétaux.

Rana, G., Katerji, N., and de Lorenzi, F. (2005). Measurement and modelling of evapotranspiration of irrigated citrus orchard under Mediterranean conditions. *Agric. For. Meteorology* 128 (3-4), 199–209. doi:10.1016/j.agrformet.2004.11.001

Rana, G., Katerji, N., Ferrara, R. M., and Martinelli, N. (2011). An operational model to estimate hourly and daily crop evapotranspiration in hilly terrain: validation on wheat and oat crops. *Theor. Appl. Climatol.* 103 (3-4), 413–426. doi:10.1007/s00704-010-0308-5

Rana, G., Katerji, N., Mastrorilli, M., and Moujabber, M. (1997a). A model for predicting actual evapotranspiration under soil water stress in a Mediterranean region. *Theor. Appl. Climatol.* 56 (1-2), 45–55. doi:10.1007/bf00863782

Rana, G., Katerji, N., Mastrorilli, M., and Moujabber, M. E. (1994). Evapotranspiration and canopy resistance of grass in a Mediterranean region. *Theor. Appl. Climatol.* 50 (1), 61–71. doi:10.1007/bf00864903

Rana, G., Katerji, N., Mastrorilli, M., Moujabber, M. E., and Brisson, N. (1997b). Validation of a model of actual evapotranspiration for water stressed soybeans. *Agric. For. Meteorology* 86 (3-4), 215–224. doi:10.1016/s0168-1923(97)00009-9

Rana, G., Katerji, N., and Perniola, M. (2001). Evapotranspiration of sweet sorghum: a general model and multilocal validity in semiarid environmental conditions. *Water Resour. Res.* 37 (12), 3237–3246. doi:10.1029/2001wr000476

Shi, T. T., Guan, D. X., Wang, A. Z., Wu, J. B., Jin, C. J., and Han, S. J. (2008). Comparison of three models to estimate evapotranspiration for a temperate mixed forest. *Hydrol. Process.* 22 (17), 3431–3443. doi:10.1002/hyp.6922

Shi, Y., Shi, H., Cui, Y., Hong, D., and Zhu, H. (2021). Variation of water use efficiency in a paddy field in the middle and lower reaches of the Yangtze River using eddy covariance method. *Trans. Chin. Soc. Agric. Eng.* 37 (4), 130–139. doi:10.11975/j.issn. 1002-6819.2021.04.016

Srivastava, R. K., Panda, R. K., Chakraborty, A., and Halder, D. (2018). Comparison of actual evapotranspiration of irrigated maize in a sub-humid region using four different canopy resistance based approaches. *Agric. Water Manag.* 202, 156–165. doi:10.1016/j. agwat.2018.02.021

Todorovic, M. (1999). Single-layer evapotranspiration model with variable canopy resistance. *J. Irrigation Drainage Eng.* 125 (5), 235–245. doi:10.1061/(asce)0733-9437(1999)125:5(235)

Xu, L., Xiao, K., and Wei, R. (2020). Irrigation models for the tomatoes cultivated in organic substrate based on greenhouse environment and crop growth. *Trans. Chin. Soc. Agric. Eng.* 36 (10), 189–196. doi:10.11975/j.issn.1002-6819.2020.10.023

Yan, H., Zhou, Y., Zhang, J., Wang, G., Zhang, C., Yu, J., et al. (2022a). Parametrization of canopy resistance and simulation of latent heat fluxes for typical crops in southern Jiangsu Province. *Trans. Chin. Soc. Agric. Eng.* 38 (9), 101–107. doi:10. 11975/j.issn.1002-6819.2022.09.011

Yan, H. F., Deng, S. S., Zhang, C., Wang, G. Q., Zhao, S., Li, M., et al. (2023). Determination of energy partition of a cucumber grown Venlo-type greenhouse in southeast China. *Agric. Water Manag.* 276, 108047. doi:10.1016/j.agwat.2022.108047

Yan, H. F., Huang, S., Zhang, J. Y., Zhang, C., Wang, G. Q., Li, L. L., et al. (2022b). Comparison of shuttleworth-wallace and dual crop coefficient method for estimating evapotranspiration of a tea field in southeast China. *Agriculture-Basel* 12 (9), 1392. doi:10.3390/agriculture12091392

Yan, H. F., Shi, H. B., Hiroki, O., Zhang, C., Xue, Z., Cai, B., et al. (2015). Modeling bulk canopy resistance from climatic variables for predicting hourly evapotranspiration of maize and buckwheat. *Meteorology Atmos. Phys.* 127 (3), 305–312. doi:10.1007/ s00703-015-0369-1

Yan, H. F., Yu, J. J., Zhang, C., Wang, G. Q., Huang, S., and Ma, J. M. (2021). Comparison of two canopy resistance models to estimate evapotranspiration for tea and wheat in southeast China. *Agric. Water Manag.* 245, 106581. doi:10.1016/j.agwat.2020.106581

Yu, J. (2022). *Characterization and simulation of water-heat flux changes in typical farmland in the southern Jiangsu region*. Jiangsu University. doi:10.27170/d.cnki.gjsuu. 2021.000315

Zhang, B., Xu, D., Liu, Y., and Chen, H. (2015). Review of multi-scale evapotranspiration estimation and spatio-temporal scale expansion. *Trans. Chin. Soc. Agric. Eng.* 31 (6), 8–16. doi:10.3969/j.issn.1002-6819.2015.06.002

Zheng, H. X., Wang, B. Y., Cao, X. S., Wu, J. B., Yan, H. F., and Tian, D. L. (2023). Optimization of subsurface drip irrigation schedule of alfalfa in Northwest China. *Water* 15 (12), 2242. doi:10.3390/w15122242